Photonics and Nanostructures - Fundamentals and Applications 51 (2022) 101045

Contents lists available at ScienceDirect

Photonics and Nanostructures - Fundamentals and Applications

journal homepage: www.elsevier.com/locate/photonics

Theoretical study of distance-dependent optical fiber SPR sensor based on MoS_2 nanosheets

Jiang Wu [a,b,1], Zhiguo Wu [c,d,1], Rohan Weerasooriya [c], Xing Chen [e], Yu Huang [a,b,*]

[a] Chongqing Institute of Green and Intelligent Technology, Chinese Academy of Sciences, Chongqing 400714, China
[b] University of Chinese Academy of Science, Beijing 100049, China
[c] National Centre for Water Quality Research, National Institute of Fundamental Studies, Hanthana, Kandy 20000, Sri Lanka
[d] Postgraduate Institute of Science, University of Peradeniya, 20400, Sri Lanka
[e] Institute of Industry and Equipment Technology, Hefei University of Technology, Hefei 230009, China

ARTICLE INFO

Keywords:
Surface plasmon resonance
Optical fiber
MoS_2 nanosheets
Distance-dependent sensing

ABSTRACT

Sandwich assay employing gold nanoparticles and DNA is a common signal amplification strategy designed for surface plasmon resonance sensor. To further improve the sensitivity employing sandwich assay, sandwich-structured optical fiber surface plasmon resonance sensors based on AuNPs and MoS_2 nanosheets has been theoretically studied. Au film deposited on fiber core is the bottom nanomaterial of sandwich structure while AuNPs and MoS_2 nanosheets are optional used as top nanomaterials. Top and bottom nanomaterials are separated by double stranded DNA, which allows solvent to perform as a spacer. The thickness of spacer is able to be tuned by the number of base pairs of double stranded DNA. Spacer thickness and nanomaterials play important roles to regulate the performance of optical fiber surface plasmon resonance sensor. The refractive index sensitivity has been found to be enhanced by the presence of MoS_2 nanosheets compared to AuNPs. Large spacer thickness supported by long double stranded DNA further improves the performance of sensor. This study yields new insight into the structural design of optical fiber surface plasmon resonance sensor enhanced by sandwich structure and will open exciting avenues to apply sandwich-like assay for biosensing.

1. Introduction

Surface plasmon resonance (SPR) sensors are important and indispensable tools in the chemical and biological fields due to their advantage of real-time, high sensitivity, label-free and rapid responsive detection [1–7]. This technology is to produce evanescent wave at thin metallic film, typically gold or silver, and a dielectric medium interface, exhibiting exponential decay of the energy transfer field intensity of surface plasmon wave. Variation in the refractive index change caused by specific interaction between receptors and target at the sensor surface leads to characteristic changes in resonant wavelength. Optical fiber SPR sensor not only inherits the advantage of traditional SPR sensor, but also presents several additionally desirable features, including miniaturization, integration and remote sensing. Despite all these advantages, fiber-based SPR sensors still requires some improvements in order to approach high stability and sensitivity.

Therefore, a wide range of methods have been proposed to improve the performance of optical fiber SPR sensor. At present, the strategies employed to enhance the sensitivity of optical fiber SPR sensor is mainly divided into two aspects. The first is shaping the optical fiber geometry to increase the interaction between the surface plasmon and fiber modes, such as a side-polished fiber, tapered fiber, grating-written fiber and de-cladded fiber [8–11]. The second is to modify the sensor surface with nanomaterials in order to implement signal amplification protocols, including using gold or magnetic nanoparticles, and various nanomaterials [12–15].

Au nanoparticles (AuNPs) are most frequently used as transducers and signal amplification labels in biosensors design, not only due to their increased binding mass, but also the increased perturbation of evanescent field. Sandwich-like bioassays have been successfully utilized onto optical fiber SPR sensing. Pollet et al. firstly proposed using AuNPs as signal enhancer on optical fiber SPR probes [16]. Loyes et al. designed optical fiber SPR aptasensor with AuNPs amplification to rapidly detect circulating breast cancer cells with LOD of 49 cells/mL [17]. With the

* Corresponding author at: Chongqing Institute of Green and Intelligent Technology, Chinese Academy of Sciences, Chongqing 400714, China.
E-mail address: huangyu@cigit.ac.cn (Y. Huang).

[1] These authors contributed equally to this work.

https://doi.org/10.1016/j.photonics.2022.101045
Received 5 November 2021; Received in revised form 29 April 2022; Accepted 21 June 2022
Available online 23 June 2022
1569-4410/

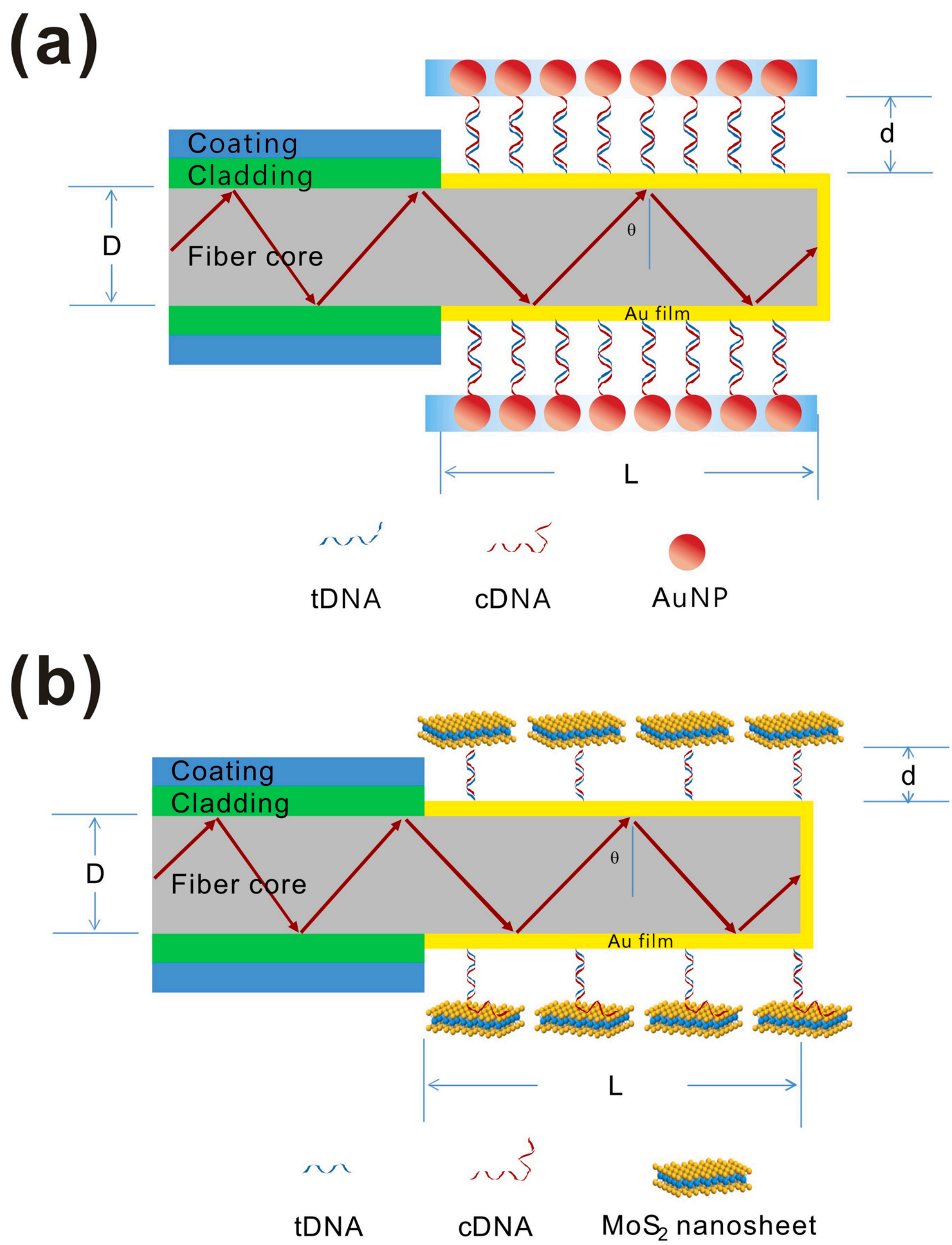

Fig. 1. Schematic diagram of optical fiber SPR sensor with (a) Au-Solvent-Au structure and (b) Au- Solvent -MoS_2 structure.

significant improvement of nanotechnology in recent years, several nanomaterials have been selected to coat on the optical fiber SPR sensor surface to enhance the sensitivity due to their enhanced SPR signal characteristics. Wei et al. introduced graphene sheets coating on gold surface of optical fiber SPR sensor and demonstrated a double increase in sensitivity compared to conventional gold film optical fiber SPR sensor [18]. More recently, molybdenum disulfide (MoS_2) nanosheet belonging to the transition-metal dichalcogenides (TMDCs) has drawn considerable attention due to its distinctive optical and electrical characteristics [19]. MoS_2 nanosheet is composed of bonded S-Mo-S through weak van der Waals force and is known as “beyond graphene” 2D nanocrystal material [20,21]. MoS_2 nanosheets can be prepared by chemical vapor deposition or liquid exfoliation methods [22,23]. Compared with graphene, MoS_2 has larger band gap and higher optical absorption efficiency, high electron mobility, larger surface to volume ratio, relatively low toxicity and good biocompatibility. Therefore, it has been successfully employed in the field of sensing, optoelectronic and energy harvesting [19,21,24]. Zeng et al. theoretically investigated that the introduction of graphene-MoS_2 hybrid structures is able to improve a phased-sensitivity enhancement factor 500 times in comparison to SPR sensing scheme without this coating [25]. Wang et al. experimentally coated MoS_2 nanosheets on the gold/silver surface of optical fiber SPR sensor and confirmed that MoS_2 has the potential to promote the refractive index sensitivity depending on the layers of MoS_2 nanosheets [26]. Kaushik et al. further reported that the MoS_2 nanosheets functionalized fiber optic SPR immunosensor exhibited better performance pathogenic detection of *Escherichia coli* compared to conventional counterpart [15].

The sandwiched structure, such as metal-insulator-metal (MIM) structure, is one of the most extensively used plasmonic-based nanostructures for the realization of sensing [27,28]. The general structure of this type of sensor is that material with low refractive index, such as air, silica, titanium dioxide, is sandwiched between two metal claddings. The resonance coupling between these two metals could achieve more harmonious and stronger, and lead spectral characteristic very sensitive to refractive index changes. However, relatively complicated fabrication increases the cost of sensor and hinders their widespread applications. At present, the structure that most MoS_2 nanosheets interfaced optical fiber SPR sensor has been studied is that MoS_2 nanosheets are directly coated with metallic film either by dip coating [15] or chemical bond [26] for quantitative analysis. Double stranded DNA (dsDNA) has been demonstrated to control the distance between donor and acceptor to design resonance energy transfer sensor [29]. Ha et al. has systematically studied fluorescence resonance energy transfer from Alexa Fluor 430 to MoS_2 nanosheets by varying the number of base pairs, which correspondingly changes the length of dsDNA and the distance between both donor and acceptor [30]. Liu et al. has proposed a distance-dependent plasmon-enhanced electrochemiluminescence biosensor that regulated the distance between MoS_2 nanosheets and gold nanoparticle through dsDNA [31]. Since the length of a single DNA base is 0.34 nm [32], the distance between donor and acceptor can be controlled by extending dsDNA bases structure. Length adjustment of dsDNA by controlling DNA bases provides an opportunity to use solvent as spacer to separate two thin nanomaterials and construct a sensor with MIM structure.

In this paper, we propose an optical fiber sensor based on two sandwich-structures with solvents placed in the interlayer, which are Au-Solvent-AuNPs (ASA) and Au-Solvent-MoS_2 (ASM) respectively, with the assistance of dsDNA to maintain separation between bottom and top nanomaterials. The sensing is performed by observing the spectral shift of ASA and ASM modes via change in refractive index of surrounding environment respectively. Since 50 nm Au film deposited on fiber core is general an approximate thickness to generate surface plasmon, so the influence of spacer thickness and properties of top nanomaterials on the performance of sensor is considered to be investigated here. Based on the theoretical results, we demonstrate that the refractive index sensitivity and differential spectra are dependent on the properties of top nanomaterials and spacer thickness. Due to the utilization of MoS_2, we show that ASM sensing is superior to that of ASA for refractive index sensing. Since sandwich-like sensing strategy based on DNA techniques is widely used in biosensing, the sensor with this proposed structure has the potential to easily fabricate and monitor target by DNA hybridization and melting.

2. Model and method

The general structure of Au-Solvent-AuNPs (ASA) sandwich-structured optical fiber sensor illustrated in Fig. 1a comprises 50 nm Au film deposited on optical fiber core as the bottom film. The second layer consists of AuNPs embedded in solvent can be approximated as a quasi-homogeneous effective-medium material, whose dielectric constant has contributions from both AuNPs and solvent. The effective medium theory proposed by Maxwell-Garnett has been proved to be a useful tool to interpret the properties of such an inhomogeneous medium. Bruggenman further improved the effective dielectric constant $\varepsilon_{\mathrm{eff}}$of such mixture of two component materials, that is expressed as [33].

$$\varepsilon_{\mathrm{eff}} = \frac{\varepsilon_i}{2(1-L_p)}\left[1-2L_p+\frac{L_p-f_p}{s} \pm \frac{\sqrt{s^2-2\left(f_p+L_p-2f_pL_p\right)s+\left(L_p-f_p\right)^2}}{s}\right] \quad (1)$$

where L_{p} is the depolarization factor determined by the shape and orientation of the particle, f_{p} is the volume fraction of metal nanoparticles within the medium and s has the form $\varepsilon_i/(\varepsilon_i - \varepsilon_p)$.$\varepsilon_i$ and $\varepsilon_p$are the dielectric constant of medium and metal particle respectively.

Considering spherical AuNPs are usually synthesized and used as signal enhancer in sandwich assay, the diameter distribution of these AuNPs is in the range from 10 to 30 nm and the thickness of this effective medium is equivalent to the diameter of AuNPs. The depolarisaiton factor L $= 1/3$ and the volume fraction p of AuNPs is 0.8 [1]. The bottom Au film and top AuNPs are connected by dsDNA composed of hybridized tDNA and cDNA. The solvent between bottom Au films and top AuNPs exerts as a spacer. Optical sensor with Au-Solvent-MoS_2 (ASM) structure is shown in Fig. 1b. The structural difference of ASM from that of ASA is that MoS_2 nanosheet is placed at the top level.

The wavelength dependent dielectric constant of core in the fiber is given by [25,34].

$$n_1(\lambda) = \sqrt{1+\frac{A_1\lambda^2}{\lambda^2-B_1^2}+\frac{A_2\lambda^2}{\lambda^2-B_2^2}+\frac{A_3\lambda^2}{\lambda^2-B_3^2}} \quad (2)$$

where Sellmeier coefficients $A_1 = 0.6961663$, $A_2 = 0.6961663$, $A_3 = 0.8774794$, $B_1 = 0.4079426$, $B_2 = 0.0684043$, $B_3 = 9.896161$ and λ is the wavelength of incident light.

The relative permittivity of gold in the sensing region is well described by Drude-Lorentz model [25].

$$\varepsilon_{DL}(\omega) = \varepsilon_\infty - \frac{\omega_D^2}{\omega(\omega+i\gamma_D)} - \frac{\Delta\varepsilon\Omega_L^2}{(\omega^2-\Omega_L^2)+i\Gamma_L\omega} \quad (3)$$

where $\omega$is the angular frequency of light, $\varepsilon_\infty$is the dimensionless high frequency limit contributed from interband transition of electrons, ω_D is plasmon frequency, γ_D is the damping coefficient due to the dispersion of the electrons, Ω_L and Γ_L are respectively the strength and spectral width of the Lorentz oscillator and $\Delta\varepsilon$ is a weight factor.

The complex refractive index of monolayer MoS_2 in the visible region is obtained from the experimental measurement data by Yim [23].

The light is launched into one end of fiber at the axial point and reflected at the opposite end. The angular reflected power distribution,dP, transmitted between θ and $\theta + d\theta$ can be expressed as [35, 36].

$$dP\alpha \frac{n_1^2\sin\theta\cos\theta}{\left(1-n_1^2\cos^2\theta\right)^2}d\theta \quad (4)$$

The normalized transmitted power of light will be derived as Eq. (5), by using the reflectance value for a single reflection at the core/Au interface

$$P = \frac{\int_{\theta=\theta_{cr}}^{\theta=\pi/2} R_p^{Nref(\theta)}\left(n_1^2\sin\theta\cos\theta\Big/\left(1-n_1^2\cos^2\theta\right)^2d\theta\right.}{\int_{\theta=\theta_{cr}}^{\theta=\pi/2}\left(n_1^2\sin\theta\cos\theta\Big/\left(1-n_1^2\cos^2\vartheta\right)^2\right)d\theta} \quad (5)$$

where$R_p = \left|r_p\right|^2$ is the reflection intensity, $Nref(\theta) = \frac{2L}{D\tan\theta}$ is the total number of light reflections performed in the fiber optic SPR sensor by a ray whose incident angle is θ with the normal to the core-Au layer interface in the sensing region with the length of L, $\theta_{cr} = 90 - a\sin\left(\frac{NA}{n_1}\right)$ is the critical angle of the fiber and NA is its numerical aperture. Because of the long distance between the input end of optical fiber and the sensitive area, the polarization effect of different launched rays is neglected.

Based on this proposed fiber optic SPR sensor structure, the parameters used for this study are numerical aperture of fiber NA= 0.22, the length of exposed sensing length L= 10 mm, fiber core diameter D= 600 μm. Considering the length of single DNA base is 0.34 nm, the distance between bottom and top nanomaterials is varied from 0 nm to 17 nm.

3. Result and discussions

It is well known that surface plasmon resonance phenomena is excited once the wave vector matching between the incident light along the direction of surface plasmon propagation and surface plasmon wave,

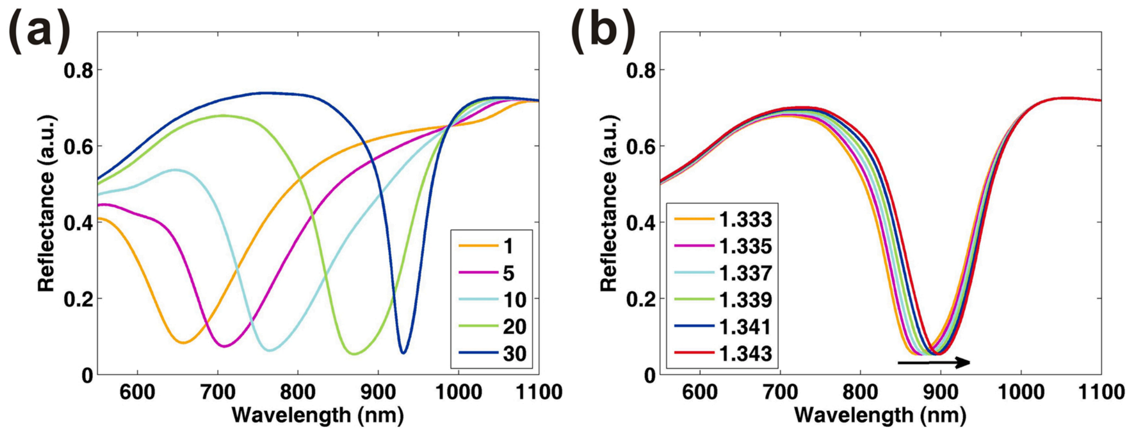

Fig. 2. Calculated reflectance spectra of Au- Solvent -MoS_2 structure with 10.2 nm spacer as a function of (a) MoS_2 layer from 1 to 30 at refractive index of 1.333 and (b) refractive index increasing from 1.333 to 1.343 at 20 layer of MoS_2 film.

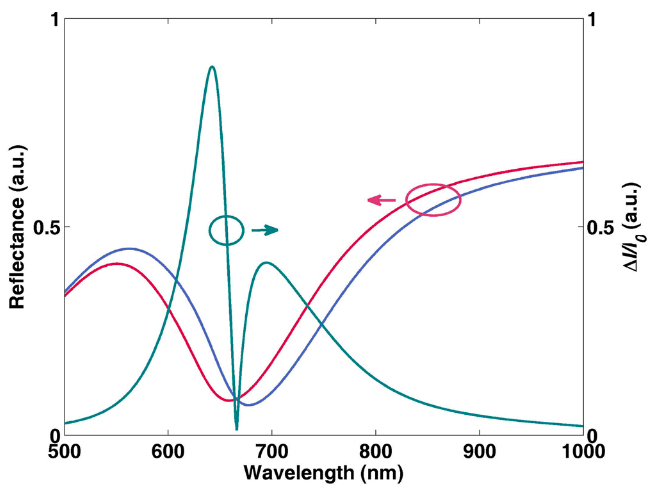

Fig. 3. Calculated reflectance spectra of optical fiber SPR sensor and corresponding differential reflectance $\Delta I/I_0$.

which is dependent on different kinds of material and ambient environment. The plasmon resonance wavelength of the sensor is depending on the type of top nanomaterial and refractive index of ambient environment. As shown in Fig. 2a, increasing MoS_2 layer number from 1 to 30 could dramatically shift the resonance wavelength from approximately 650 nm to 930 nm and narrow the spectral full width and half maximum. Large value of the real part of the dielectric function of MoS_2 is attributed to this spectral shift. At a certain MoS_2 layer number, changing refractive index from 1.333 to 1.343 is also able to perturb the resonance wavelength to longer wavelength as illustrated in Fig. 2b.

The refractive index sensitivity of optical fiber SPR sensor with wavelength interrogation is then defined as the resonance wavelength shifted by change of refractive index in surrounding environment,

$$S_n = \frac{\delta\lambda_{res}}{\delta n_s} \tag{5}$$

where δn_s is the change in refractive index of solution and $\delta\lambda_{res}$is the corresponding resonance wavelength shift.

Meanwhile, Fig. 3 gives the differential reflectance $\Delta I/I_0$ defined as

$$\Delta I/I_0 = |I_1 - I_0|/I_0 \tag{6}$$

where $I_1$and I_0represent the reflectance perturbed by higher and lower refractive index of ambient environment respectively. The introduction

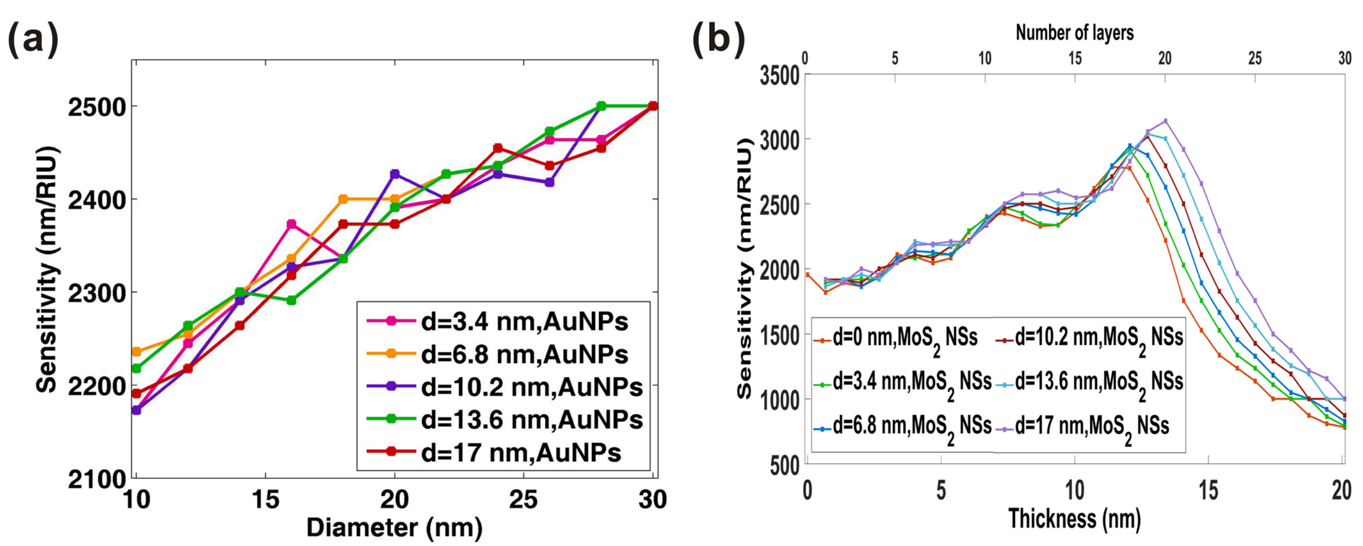

Fig. 4. (a) Refractive index sensitivity of ASA optical fiber SPR sensor as a function of AuNPs diameter at varying spacer thickness. (b) Refractive index sensitivity of ASM optical fiber SPR sensor as a function of top MoS_2 nanosheets thickness at varying spacer thickness.

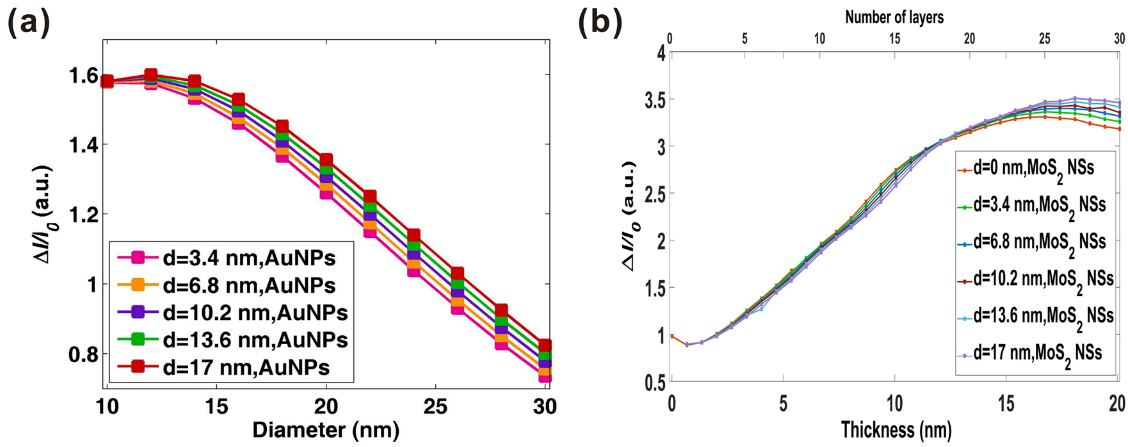

Fig. 5. (a) Maximum differential reflectance of ASA optical fiber SPR sensor as a function of top AuNPs diameter at varying spacer thickness. (b) Maximum differential reflectance of ASM optical fiber SPR sensor as a function of top MoS_2 nanosheets thickness at varying spacer thickness.

of $\Delta I/I_0$ provides a flexibility to implement single wavelength monitoring scheme that the reflectance at one single wavelength is recorded and establish a proportional relationship with the concentration of analyte.

MoS_2 is a high dielectric constant material and can enhance the electric field strength of the surface of optical fiber sensor. Consequently, the sensitivity of the optical fiber SPR sensor could be directly improved. Solvent is proposed to present between bottom and top nanomaterials supported by dsDNA in this study. Then, the research work on the influence of MoS_2 associated with spacer thickness is analyzed. The influence of these factors, including the layer number of MoS_2 nanosheets, the distance between Au films and AuNPs for ASA, the distance between Au film and MoS_2 nanosheets for ASM, on the refractive index sensitivity S_n and differential reflectance $\Delta I/I_0$ in the range from 1.333 to 1.343 are taking into consideration. Fig. 4a and b present the refractive index sensitivity with varying AuNPs diameters for ASA and layer numbers of MoS_2 nanosheets for ASM respectively. It is noted that increasing in AuNPs diameter from 10 to 30 nm is able to gradually increase the sensitivity at a certain distance between Au film and AuNPs from 2200 to 2500 nm/RIU. However, enlarging the gap between these two nanomaterials from 3.4 to 17 nm has negligible effect on the sensitivity improvement. Comparing to that of ASA structure, optical fiber sensor with ASM structure exhibits a different performance. As layer number of MoS_2 increases, the refractive index sensitivity slightly increases and reaches a peak at approximate 18–20 layers regardless of the distance between bottom Au film and top MoS_2 nanosheets. Then, it turns to decrease with increasing MoS_2 layer number to 30. Furthermore, the pronounced dependence of sensitivity on distance is more obvious when the layer number of MoS_2 nanosheet is larger than 18. 17 nm distance between bottom Au film and top MoS_2 nanosheets could lead the sensitivity to be the highest in this category.

Fig. 5a depicts the maximum differential reflectance $\Delta I/I_0$ as a function of AuNPs diameters for ASA structure. It is clearly visible that the maximum $\Delta I/I_0$ exhibits a slight increase followed by a sharp decrease with the increase of AuNPs diameter from 10 to 30 nm, and approximately 12 nm AuNPs would produces the highest value. The effect of distance on $\Delta I/I_0$ becomes clearer at larger diameter of AuNPs. In contrast, maximum $\Delta I/I_0$ for ASM structure shown in Fig. 5b gradually approaches a plateaus when the layer number of MoS_2 film increases to approximately 25–27. In addition, ASM structural sensor with 17 nm gap between bottom Au film and top MoS_2 nanosheets also shows a slightly higher maximum $\Delta I/I_0$ compared to sensor constituting of other gaps. By comparing the maximum $\Delta I/I_0$ resulted from ASA structure and ASM structure, maximum $\Delta I/I_0$ produced by ASM structure always produce better performance than that of ASA structure, which is in accordance with that of refractive index sensitivity contributed from MoS_2.

The use of AuNPs as signal enhancer in sandwich assay is a well-known technique. Their mass effect and local refractive index change is the first reason for the signal enhancement. The second is electromagnetic field enhancement resulting in higher sensitivity. Only AuNPs presents within the range of evanescent wave into the external medium emerging from Au film surface can produce electromagnetic coupling. Therefore, it is found that increasing AuNPs diameters equivalent to

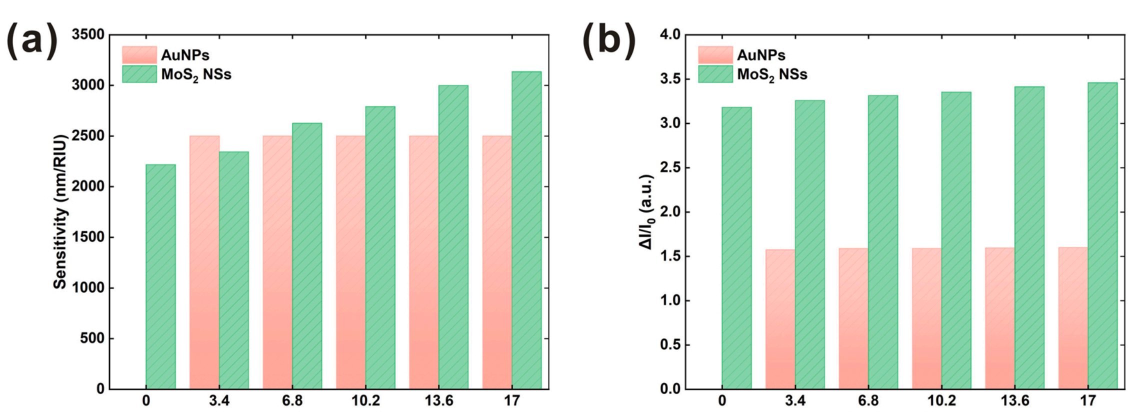

Fig. 6. (a) Sensitivity comparison for ASA (AuNPs diameter = 30 nm) and ASM (layer number of MoS_2 nanosheets = 20) optical fiber SPR sensor. (b) Differential reflectance comparison for ASA (AuNPs diameter = 12 nm) and ASM (layer number of MoS_2 nanosheets = 27) optical fiber SPR sensor.

increasing their mass of AuNPs, and their mass dominates the role of sensitivity amplifier for ASA structure, while the spacer thickness have negligible effect. By contrast, both increasing the layer number of MoS_2 nanosheets and spacer thickness at a certain value in ASM structure could significantly enhance the sensitivity and differential reflectance. This confirms two main effects, including a chemical enhancement due to the nature of MoS_2 nanosheets and associated electromagnetic coupling, yield this higher sensitivity.

In order to analyze the influence of spacer thickness on the refractive index sensitivity and differential reflectance, Fig. 6a shows the sensitivity selected from the best ASA structure (AuNPs diameter =30 nm) and ASM structure (layer number of $MoS_2 =$ 20), which could produce highest sensitivity, as a function of gap distance. Although sensitivity produced by MoS_2 nanosheets is smaller than that produced by AuNPs in the case of 0 and 3.4 nm gap distance, it surpasses that of AuNPs once gap distance is enlarged than 6.8 nm. In the case of MoS_2 nanosheets as the top nanomaterial, sensitivity increases by 41.38% when the distance is 17 nm thick compared to that of MoS_2 nanosheets directly attached on the Au film. Not surprisingly, the spacer has little effect on the sensitivity of sensor with AuNPs as top nanomaterial. Similar behaviour is observed for $\Delta I/I_0$ as illustrated in Fig. 6b. $\Delta I/I_0$ produced by ASA structure with 12 nm AuNPs diameter and ASM structure with 27 layer of MoS_2 are compared here. Gap distance of 17 nm for sensor comprising of MoS_2 nanosheets produces nearly 8.71% improvement of $\Delta I/I_0$ in comparison to that of direct attachment of MoS_2 nanosheets. Moreover, large distance between MoS_2 nanosheet and Au film always produces better refractive index sensitivity and $\Delta I/I_0$ than that of AuNPs, which demonstrates the spacer thickness is an important parameter to design ASM structured optical fiber SPR sensor and confirms its advantage for sensing.

4. Conclusions

A SPR based optical fiber sensor with ASA and ASM structure have been theoretically analyzed and compared. The analysis of sensor's performance is carried out in terms of its refractive index sensitivity and differential reflectance. The presence of MoS_2 nanosheets as top nanomaterials in ASM structure could provide better sensitivity and differential reflectance compared to that of AuNPs as top nanomaterials in ASA structure. The sensitivity and differential reflectance increases with an increase in gap distance between bottom Au film and top MoS_2 nanosheets in ASM structure. It is further investigated that the sensitivity and differential reflectance could approach best value at a certain layer number of MoS_2 nanosheets. Hence, the proposed fiber SPR sensor based on ASM structure has a potential to be constructed due to the use of dsDNA and applied in a broad biosensing field.

Declaration of Competing Interest

The authors declare that they have no known competing financial interests or personal relationships that could have appeared to influence the work reported in this paper.

Acknowledgments

This work is sponsored by the Natural Science Foundation of Chongqing (Grant No. cstc2018jcyjAX0718).

References

[1] Y. Huang, M.C. Pitter, M.G. Somekh, W. Zhang, W. Xie, H. Zhang, H. Wang, S. Fang, Plasmonic response of gold film to potential perturbation, Sci. China Phys. Mech. 56 (2013) 1495–1503.
[2] Y. Huang, M.C. Pitter, M.G. Somekh, Time-dependent scattering of ultrathin gold film under potential perturbation, ACS Appl. Mater. Inter. 4 (2012) 3829–3836.
[3] Y. Huang, M.C. Pitter, M.G. Somekh, Morphology-dependent voltage sensitivity of a gold nanostructure, Langmuir 27 (2011) 13950–13961.
[4] J. Wu, Y. Huang, X. Bian, D. Li, Q. Cheng, S. Ding, Biosensing of BCR/ABL fusion gene using an intensity-interrogation surface plasmon resonance imaging system, Opt. Commun. 377 (2016) 24–32.
[5] B.R. Heidemann, I. Chiamenti, M.M. Oliveira, M. Muller, J.L. Fabris, Plasmonic optical fiber sensors: enhanced sensitivity in water-based environments, Appl. Opt. 54 (2015) 8192–8197.
[6] T. Shigeru, S. Atsumu, Y. Yasuhiko, Y. Shigeru, I. Yoshihito, Surface design of SPR-based immunosensor for the effective binding of antigen or antibody in the evanescent field using mixed polymer matrix, Sens. Actuators B Chem. 52 (1998) 65–71.
[7] Y. Shevchenko, G. Camci-Unal, D.E. Cuttica, M.R. Dokmeci, J. Albert, A. Khademhosseini, Surface plasmon resonance fiber sensor for real-time and label-free monitoring of cellular behavior, Biosens. Bioelectron. 56 (2014) 359–367.
[8] Y. Xu, Z.W. Luo, J.M. Chen, Z.J. Huang, X. Wang, H.F. An, Y.X. Duan, Omega-shaped fiber-optic probe-based localized surface plasmon resonance biosensor for real-time detection of salmonella typhimurium, Anal. Chem. 90 (2018) 13640–13646.
[9] D.W. Kim, Y. Zhang, K.L. Cooper, In-fiber reflection mode interferometer based on a long-period grating for external refractive-index measurement, Appl. Opt. 44 (2005) 5368–5373.
[10] Y. Zhao, R.J. Tong, F. Xia, Y. Peng, Current status of optical fiber biosensor based on surface plasmon resonance, Biosens. Bioelectron. 142 (2019), 111505.
[11] N. Goswami, K.K. Chauhan, A. Saha, Analysis of surface plasmon resonance based bimetal coated tapered fiber optic sensor with enhanced sensitivity through radially polarized light, Opt. Commun. 379 (2016) 6–12.
[12] C. Zhou, H.M. Zou, M. Li, C.J. Sun, D.X. Ren, Y.X. Li, Fiber optic surface plasmon resonance sensor for detection of E. coli O157:H7 based on antimicrobial peptides and AgNPs-rGO, Biosens. Bioelectron. 117 (2018) 347–353.
[13] A.M. Shrivastav, B.D. Gupta, SPR and molecular imprinting-based fiber-optic melamine sensor with high sensitivity and low limit of detection, Ieee. J. Sel. Top. Quant. 22 (2016) 172–178.
[14] S.P. Usha, A.M. Shrivastav, B.D. Gupta, FO-SPR based dextrose sensor using Ag/ZnO nanorods/GOx for insulinoma detection, Biosens. Bioelectron. 85 (2016) 986–995.
[15] S. Kaushik, U.K. Tiwari, S.S. Pal, R.K. Sinha, Rapid detection of Escherichia coli using fiber optic surface plasmon resonance immunosensor based on biofunctionalized Molybdenum disulfide (MoS2) nanosheets, Biosens. Bioelectron. 126 (2019) 501–509.
[16] I. Arghir, F. Delport, D. Spasic, J. Lammertyn, Smart design of fiber optic surfaces for improved plasmonic biosensing, N. Biotech. 32 (2015) 473–484.
[17] M. Loyez, E.M. Hassan, M. Lobry, F. Liu, C. Caucheteur, R. Wattiez, M.C. DeRosa, W.G. Willmore, J. Albert, Rapid detection of circulating breast cancer cells using a multiresonant optical fiber aptasensor with plasmonic amplification, ACS Sens. 5 (2020) 454–463.
[18] W. Wei, J. Nong, Y. Zhu, G. Zhang, N. Wang, S. Luo, N. Chen, G. Lan, C.-J. Chuang, Y. Huang, Graphene/Au-enhanced plastic clad silica fiber optic surface plasmon resonance sensor, Plasmonics 13 (2017) 483–491.
[19] J. Chao, M. Zou, C. Zhang, H. Sun, D. Pan, H. Pei, S. Su, L. Yuwen, C. Fan, L. Wang, A MoS(2)-based system for efficient immobilization of hemoglobin and biosensing applications, Nanotechnology 26 (2015), 274005.
[20] Y. Zhao, Y. Huang, J. Wu, X. Zhan, Y. Xie, D. Tang, H. Cao, W. Yun, Mixed-solvent liquid exfoliated MoS2 NPs as peroxidase mimetics for colorimetric detection of H2O2 and glucose, RSC Adv. 8 (2018) 7252–7259.
[21] A.K. Singh, P. Kumar, D.J. Late, A. Kumar, S. Patel, J. Singh, 2D layered transition metal dichalcogenides (MoS2): synthesis, applications and theoretical aspects, Appl. Mater. Today 13 (2018) 242–270.
[22] J.N. Coleman, M. Lotya, A. O'Neill, Two-dimensional nanosheets produced by liquid exfoliation of layered, Mater. Sci. 331 (2011) 568–571.
[23] C.Y. Yim, M. O''Brien, N. Mcevoy, S. Winters, I. Mirza, J.G. Luney, G.S. Duesberg, Investigation of the optical properties of MoS2 thin films using spectroscopic ellipsometry, Appl. Phys. Lett. 104 (2014) 10451.
[24] M. Kukkar, G.C. Mohanta, S.K. Tuteja, P. Kumar, A.S. Bhadwal, P. Samaddar, K. H. Kin, A. Deep, A comprehensive review on nano-molybdenum disulfide/DNA interfaces as emerging biosensing platforms, Biosens. Bioelectron. 107 (2018), 244-25.
[25] W. Wei, J.P. Nong, L.L. Tang, N. Wang, C.J. Chuang, Y. Huang, Graphene-MoS2 hybrid structure enhanced fiber optic surface plasmon resonance sensor, Plasmonics 12 (2017) 1205–1212.
[26] Q. Wang, X. Jiang, L.Y. Niu, X.C. Fan, Enhanced sensitivity of bimetallic optical fiber SPR sensor based on MoS2 nanosheets, Opt. Lasers Eng. 128 (2020), 105997.
[27] T.P. Xu, Z.X. Geng, Strategies to improve performances of LSPR biosensing: structure, materials, and interface modification, Biosens. Bioelectron. 174 (2021), 112850.
[28] N.L. Kazanskiy, S.N. Khonina, M.A. Butt, Plasmonic sensors based on Metal-insulator-metal waveguides for refractive index sensing applications: a brief review, Phys. E Low. Dimens. Syst. Nanostruct. 117 (2020), 113798.
[29] Y. Cao, T. Xie, R.C. Qian, Y.T. Long, Plasmon resonance energy transfer: coupling between chromophore molecules and metallic nanoparticles, Small 13 (2017), 1601955.
[30] H.D. Ha, D.J. Ha, J.S. Choi, M. Park, T.S. Seo, Dual role of blue luminescent MoS2 quantum dots in fluorescence resonance energy transfer phenomenon, Small 10 (2014) 3858–3862.
[31] Y. Liu, Y. Nie, M.K. Wang, Q. Zha, g Q. Ma, Distance-dependent plasmon-enhanced electrochemiluminescence biosensor based on MoS2 nanosheets, Biosens. Bioelectron. 148 (2019), 111823.

[32] S. Ghosh, D. Datta, M. Cheema, M. Dutta, M.A. Stroscio, Aptasensor based optical detection of glycated albumin for diabetes mellitus diagnosis, Nanotechnology 28 (2017), 435505.
[33] L. Gao, L.P. Gu, Y.Y. Huang, Effective medium approximation for optical bistability in nonlinear metal-dielectric composites, Solid State Commun. 129 (2004) 593–598.
[34] Y. Huang, D. Wu, C.,J. Chuang, B. Nie, H.L. Cui, W. Yun, Theoretical analysis of tapered fiber optic surface plasmon resonance sensor for voltage sensitivity, Opt. Fiber Technol. 22 (2015) 42–45.
[35] A.K. Sharma, B.D. Gupta, On the sensitivity and signal to noise ratio of a step-index fiber optic surface plasmon resonance sensor with bimetallic layers, Opt. Commun. 245 (2005) 159–169.
[36] Y. Huang, L.P. Xia, W. Wei, C.J. Chuang, C.L. Du, Theoretical investigation of voltage sensitivity enhancement for surface plasmon resonance based optical fiber sensor with a bimetallic layer, Opt. Commun. 333 (2014) 146–150.